Cellulose (2010) 17:595–606
DOI 10.1007/s10570-010-9403-0

Cellulose nanofibers from white and naturally colored cotton fibers

Eliangela de Morais Teixeira · Ana Carolina Corrêa · Alexandra Manzoli · Fabio de Lima Leite · Cauê Ribeiro de Oliveira · Luiz Henrique Capparelli Mattoso

Received: 8 September 2009 / Accepted: 29 January 2010 / Published online: 12 February 2010

Abstract Suspensions of white and colored nanofibers were obtained by the acid hydrolysis of white and naturally colored cotton fibers. Possible differences among them in morphology and other characteristics were investigated. The original fibers were subjected to chemical analysis (cellulose, lignin and hemicellulose content), X-ray diffraction (XRD) analysis, and scanning electron microscopy (SEM). The nanofibers were analyzed with respect to yield, elemental composition (to assess the presence of sulfur), zeta potential, morphology (by scanning transmission electron microscopy (STEM)) and atomic force microscopy (AFM), crystallinity (XRD) and thermal stability by thermogravimetric analysis in air under dynamic and isothermal temperature conditions. Morphological study of several cotton nanofibers showed a length of 85–225 nm and diameter of 6–18 nm. The micrographs also indicated that there were no significant morphological differences among the nanostructures from different cotton fibers. The main differences found were the slightly higher yield, sulfonation effectiveness and thermal stability under dynamic temperature conditions of the white nanofiber. On the other hand, in isothermal conditions at 180 °C, the colored nanofibers showed a better thermal stability than the white.

Keywords Naturally colored cotton fibers · Colored cellulose nanofibers · AFM · STEM

Abbreviations

CW	White cellulose
CB	Brown cellulose
CG	Green cellulose
CR	Ruby cellulose
CNW	White nanocellulose
CNB	Brown nanocellulose
CNG	Green nanocellulose
CNR	Ruby nanocellulsoe

Introduction

Natural cotton fibers (*Gossypium hirsutum* L.) are normally white but naturally colored cotton can be produced by genetic breeding techniques, avoiding

E. de Morais Teixeira (✉) · A. C. Corrêa · A. Manzoli · F. de Lima Leite · C. R. de Oliveira · L. H. C. Mattoso
National Nanotechnology Laboratory for Agribusiness (LNNA), Embrapa Agricultural Instrumentation, P.O. Box 741, São Carlos, SP 13560-970, Brazil
e-mail: eliangelat@yahoo.com.br

A. C. Corrêa
Federal University of Sao Carlos (UFSCar), via Washington Luiz, km 235, Monjolinho, P.O. Box 676, Sao Carlos, SP 13565-905, Brazil

F. de Lima Leite
Federal University of Sao Carlos (UFSCar), Rodovia João Leme dos Santos, km 110 (SP 264), P.O. Box: 3031, Sorocaba, SP 18052-780, Brazil

the need for synthetic dyes that may pollute the environmental and affect human health. Additionally, the elimination of chemical dyeing from textile manufacturing could make the product cheaper (Zhu et al. 2006).

Colored cottons were cultivated and used as long ago as 2300 B.C. in South and Central America (Murthy 2001). These are regarded as inferior to white cotton, in virtue of the lower yield, shorter and weaker fibers and variably of the color. Hence, cotton breeders are trying to improve these characteristics to produce better and more productive varieties of colored cotton (Murthy 2001; Dutt et al. 2004). Commercially, the colored fibers gained greater prominence after the impressive efforts made by Sally Fox to improve the fiber quality of colored cottons by selective breeding, resulting in colored hybrids able to produce machine-spinnable colored cotton (Murthy 2001). Currently, researchers have developed the breeding program, to encompass studies on the structure, quality, chemistry, color measurement and standardization of colored cottons (Rodgers et al. 2008). Applications such as ecological textile products have been promoted by the United States Department of Agriculture—Agricultural Research Service (USDA-ARS) (Chen et al. 2004). Specifically the Cotton Division National Agency for Advancement of Agribusiness (EMBRAPA Algodão, Brazil), has been developing novel colored cotton cultivars in their breeding program (Rocha et al. 2008).

It has been shown experimentally that the pigments in naturally colored fibers might be flavonoid compounds, such as flavonone, flavonol and anthocyanidin (Xiao et al. 2007; Hua et al. 2007). The color is controlled by a dominant gene (the genetic factor) and environmental factors that influence mainly the intensity of the color (De Carvalho and dos Santos 2003; Xiao et al. 2007), but the identities of the pigments in colored fibers are essentially unknown yet.

Nowadays, there is growing interest in the use of more environment-friendly materials and polymers of natural occurrence, such as cellulose, have had a lot of attention from those endeavoring to develop materials, especially as reinforcement in polymer matrices. Cellulose is a versatile polymer that can be extracted in a nanofiber form. Needle-like cellulose nanofibers (known as whiskers) have been studied intensively, owing to their high performance when used as reinforcement in polymer matrices to produce "green" nanocomposites (Samir et al. 2005; Bhatnagar and Sain 2005; Gardner et al. 2008). In brief, one way of obtaining such nanofibers is by acid hydrolysis the cellulose being exposed to sulfuric acid for a controlled period of time and temperature. This process removes the amorphous parts of the cellulose, leaving single and well-defined crystals in a stable colloidal suspension and promotes the grafting of sulfate groups on cellulose microfibril surface. The stability of this suspension is due to the electrostatic repulsion between the negative sulfate groups on the surface of nanofibers (Lima and Borsali 2004; Dufresne 2006).

The geometric properties of the nanocellulose structures (shape, length and diameter) depend mainly on the origin of the cellulose and the extraction process (acid hydrolysis, shearing and high-pressure homogenization, biosynthesis by bacteria or electrospinning). Several sources of cellulose have been used to obtain cellulose nanostructures, not necessarily needle-shaped, which have high crystallinity. Examples include tunicin (Anglès and Dufresne 2000, 2001), wheat straw (Alemdar and Sain 2008), bacterial cellulose (Nakagaito et al. 2005, sisal De Rodriguez et al. 2006; Morán et al. 2008), banana residues (Zuluaga et al. 2007; Cherian et al. 2008), hemp (Bhatnagar and Sain 2005) and microcrystalline cellulose (Wang et al. 2007b). Recently, cellulose nanoparticles have been also synthesized in spherical form (Pu et al. 2007; Zhang et al. 2007, 2008).

Conventional cotton nanocellulose obtained from white microcrystalline fibers has been studied by several authors (Dong et al. 1998; Orts et al. 2005; Wang et al. 2006; Medeiros et al. 2008).

In this study, fibers and nanofibers extracted from white and naturally colored cotton (brown, green and ruby) were characterized in terms of chemical composition, (content of cellulose, lignin, hemicellulose and elemental analysis), zeta potential, morphology (SEM for fibers, STEM and AFM for nanofibers), crystallinity (XRD) and thermal stability (TG). The original colored fibers were developed by Empresa Brasileira de Pesquisa Agropecuária (EMBRAPA Algodão, Brazil).

Experimental

Materials

White (commercial type) (CW) and colored cotton fibers were supplied by Embrapa Algodão (Campina Grande, Paraiba, Brazil). The colored fibers employed were: brown (CB), green (CG) and ruby (CR). Aqueous 72 wt% sulfuric acid (Synth), 17.5 wt% aqueous NaOH solution (Qhemis), sodium chlorite ($NaClO_2$, J. T. Baker) and glacial acetic acid (Synth) were used to determine the chemical composition of the fibers. Cellulose was hydrolyzed with 6.5 M sulfuric acid (Synth) and cellulose membrane (Sigma–Aldrich: D9402) was used to dialyze the products.

Methods

Chemical composition of original cotton fibers

The cotton fibers were finely chopped in a knife mill, passed through a 10-mesh sieve, dewaxed with 1:1 (v/v) ethanol:cyclohexane (Synth) for 12 h in a soxhlet apparatus and then vigorously washed with tap water. The dewaxed samples were dried for 12 h at 100 °C in an air-circulating oven. The colored cotton fibers were not discolored by this treatment.

The lignin content of the fibers was analyzed by reaction with sulfuric acid, using a standard method recommended in TAPPI-T222 om-88, and the holocellulose (cellulose + hemicelluloses) content was determined as described in TAPPI T19m-54. The α-cellulose was removed from the holocellulose by alkali extraction and the hemicellulose content was found by subtracting the α-cellulose part from the holocellulose content. The average of three replicates was calculated for each cotton fiber sample.

Preparation of the cellulose nanofibers, yield and total sulfur content

Except for the dewaxing treatment, the cotton fibers were used without any type of bleaching. About 5.0 g of fibers were dispersed in 100 mL of 6.5 M sulfuric acid at 45 °C and stirred vigorously for 75 min. After that, 500 mL of cold distilled water was added to stop the reaction. The sulfuric acid was partially removed from the resulting suspension by centrifugation at 10,000 rpm for 10 min. The non reactive sulfate groups are removed by centrifugation following by dialysis. Them the fibers were resuspended and dialyzed against tap water with a cellulose membrane, until the pH reached 6–7. The resulting suspension was ultrasonicated for 5 min and stored in a refrigerator after the addition of drops of chloroform. Nanofiber suspensions were labeled CNW, CNB, CNG and CNR, according to the cotton fibers used—CW, CB, CG and CR, respectively. For elemental analysis, XRD and TG an aliquot of 25 mL for each analysis was drying at 35 °C for 12 h in an air-circulating oven.

The yield of cellulose nanofibers was determined by weighing a 10 mL aliquot of the suspension after standing overnight to dry. Yield (%) and concentration (g mL^{-1}) were calculated from the difference between initial and final weight.

Elemental analysis was performed mainly to determine the total sulphur content before and after the extraction of nanofibers. It was carried out with EA1110-CHNS-O elemental analyzer from a CE Instruments.

Zeta potential

Electrophoretic mobilities of aliquots of aqueous nanocellulose suspensions (concentration equalized to 0.005 wt%) were measured with a Malverne 3000 Zetasizer NanoZS, (Malverne Instruments, UK).

Microscopic analyses

Scanning electron microscopy The morphology of each cotton fiber was examined under a Zeiss DSM 960 microscope. A drop of aqueous dispersed suspension of each fiber was dried and a thin layer (ca. 15 nm) of gold was sputtered on the surface.

Scanning transmission electron microscopy Nanofiber samples for scanning transmission electron microscopy (STEM) were examined in Tecnai^{TM} G2 F20 equipment. The images were acquired with a bright-field (BF) detector. A droplet of diluted suspension was deposited on a carbon microgrid (400 mesh) and allowed to dry. The grid was stained with a 1.5% solution of uranyl acetate and dried at room temperature.

Atomic force microscopy The Atomic force microscopy (AFM) measurements were performed with a Dimension V (Veeco) atomic force microscope. All images were obtained in tapping mode with a scan rate of 1 Hz, using Si tips with a radius of curvature of 11 ± 3 nm and angle of sloping tip wall about 10° (experimental values obtained with a Zeiss Supra™, FEG-SEM microscope), attached to a cantilever (*T*-shape) of spring constant 42 ± 5 N m^{-1}. The tapping amplitude was less than 4 nm and tip-sample contact time was minimal, so as to minimize the force exerted on the sample and therefore the influence of the scan on the aggregate morphology. A drop of diluted aqueous suspension of nanofibers was placed on an optical glass substrate, allowed to dry at room temperature for 12 h and then analyzed by AFM.

X-ray diffraction

The X-ray diffraction (XRD) patterns were measured for raw cotton fibers and their respective nanofibers with an X-ray diffractometer (VEB Carl Zeiss-Jena URD-6 Universal Diffractometer), using CuKα radiation ($\lambda = 1.5406$ Å) at 40 kV and 20 mA. Scattered radiation was detected in the range of $2\theta = 5$–40°, at a scan rate of 2°/min. The crystallinity index (C_I) was calculated from the heights of the 200 peak (I_{200}, $2\theta = 22.6°$) and the intensity minimum between the 200 and 110 peaks (I_{am}, $2\theta = 18°$), by means of Buschle-Diller-Zeronian equation (Eq. 1) (Buschle-Diller and Zeronian 1992). I_{200} represents both crystalline and amorphous material while I_{am} represents the amorphous material.

$$C_I(\%) = \left(1 - \frac{I_{am}}{I_{200}}\right) \times 100 \quad (1)$$

Thermogravimetric analysis

Dried fibers and nanofibers were subjected to Thermogravimetric analysis (TG) in a TA Q500 thermal analyzer (TA Instruments, New Castle, DE, USA). The samples (10.0 ± 1.0 mg) were heated in a Pt crucible from 25 to 900 °C in air flowing at 60 mL min^{-1}. The heating rate was 10 °C min^{-1}. The thermal stability of nanofibers in air was also investigated under isothermal conditions at 180 °C for 60 min, with the same heating and flow rate as above.

Results and discussion

The contents of the main constituents (hemicellulose, lignin and cellulose) of white and colored cotton fibers are presented in Table 1. These data show the presence of greater amounts of lignin and hemicellulose in the colored than in the white fibers. The green fibers had the highest total lignin content, while the ruby had the most hemicellulose. The brown fibers had intermediate contents of all these constituents, compared to the other fibers. White fibers had the highest cellulose content (about 20–25% higher than colored fibers) while ruby fibers had the lowest. The colored fibers have lower cellulose contents than white fibers because in the colored fibers carbohydrates which could have been used for cellulose synthesis may have been consumed in the synthesis of flavonoid pigments (Dutt et al. 2004; Hua et al. 2007).

The yields of the various cotton nanocelluloses were around 65 wt% for white nanofibers and 52 wt% for others. The concentration of the suspension was a little higher for CNW (0.007 g mL^{-1}) than for the colored suspensions (0.005 g mL^{-1}). As expected there was a tendency for the yield and concentration to increase with the cellulose content of the cotton.

Figure 1 shows the SEM images of raw cotton fibers and their respective original appearance at two magnifications (50× and 5,000×) The initial raw cotton fibers had a length around 500–1,000 μm and diameter of microfibrillar aggregation 13–22 μm.

After acid hydrolysis, the suspensions of the resulting nanofibers were stable and they tended to have the same color as the respective cotton fiber as shown in Fig. 2. This result shows that the pigmentation of raw colored fibers was not appreciably

Table 1 Fractions of principal constituents of white and colored cotton fibers

Fiber	White (CW)	Brown (CB)	Green (CG)	Ruby (CR)
Hemicellulose (%)	0.5 ± 0.4	9.9 ± 0.4	8.7 ± 0.9	11 ± 3.0
Cellulose (%)	97.7 ± 2.2	78.7 ± 0.4	80.3 ± 0.8	74.0 ± 2.0
Total lignin (%)	0.4 ± 0.1	9.9 ± 0.1	16.0 ± 2.0	13.8 ± 0.1

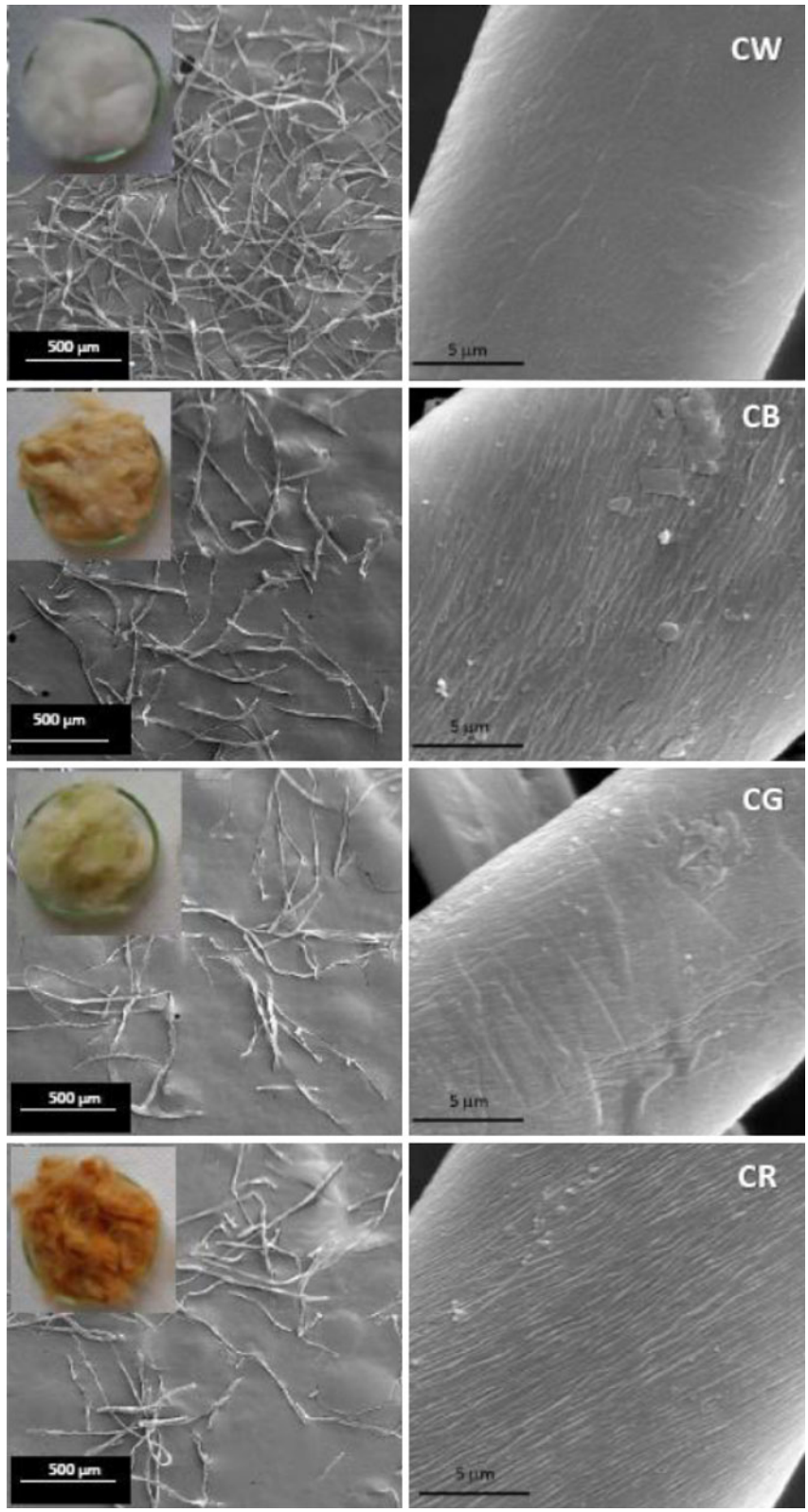

Fig. 1 Raw cotton fibers (inset) and their respective scanning electron micrographs at two magnifications

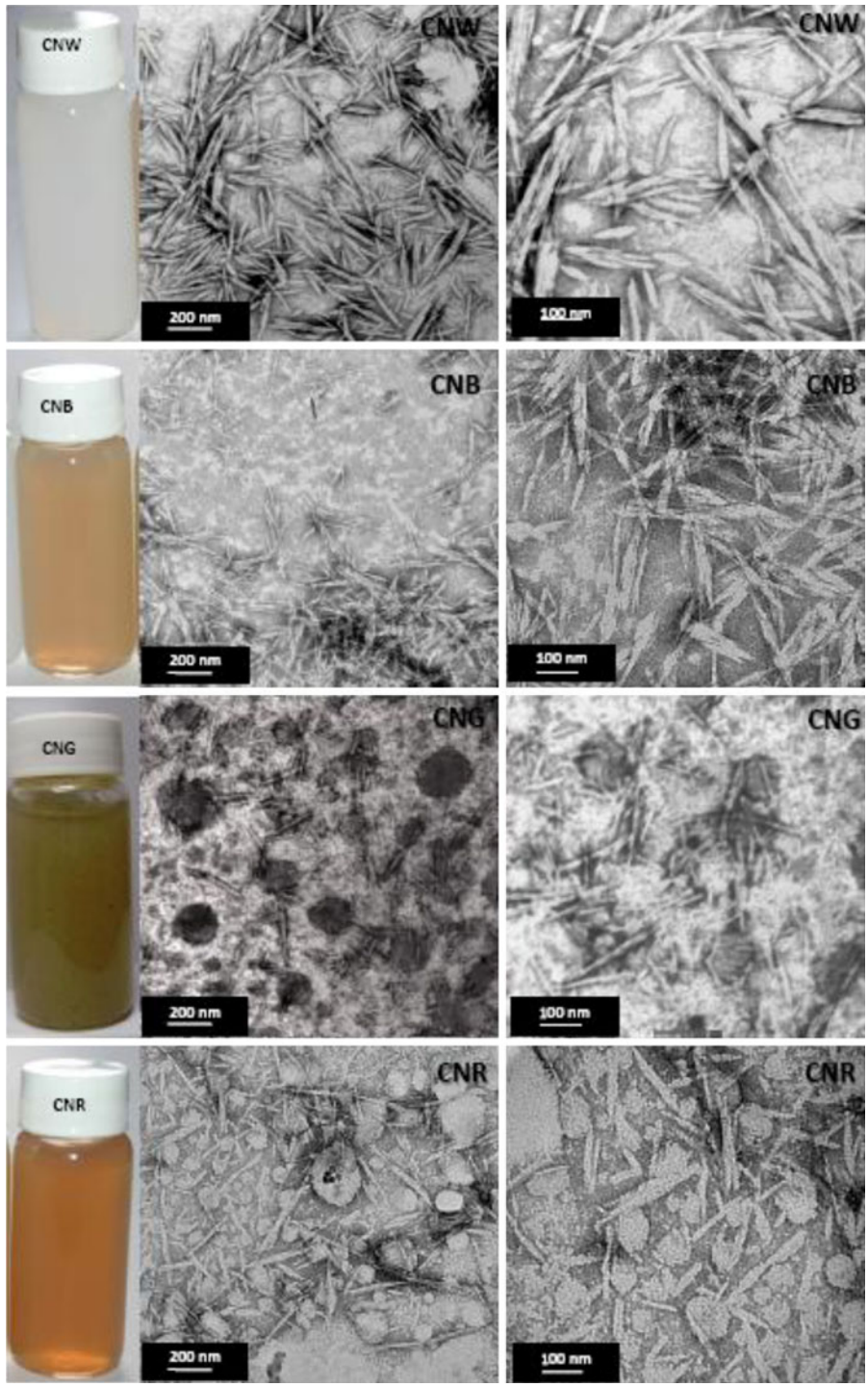

Fig. 2 Suspensions of cellulose nanofibers (*on the left*) and transmission electron micrographs of nanofibers (at two magnifications). Samples identified in the inset of the figure

affected by the acid hydrolysis and consequently these nanofibers can be used to make naturally colored plastics without the use of synthetic dyes. STEM observations (Fig. 2) showed the individual nanofibers obtained after the acid extraction. No significant difference in length or diameter could be detected by STEM among the nanofibers of various colors, if the standard deviation of each value is taken

into account (Table 2). These dimensions were calculated with the ImageJ software from about 100 nanofibers. These values are consistent with those obtained for white cotton nanofibers in the literature (Dong et al. 1998; Dufresne 2006).

Typical tapping mode AFM images, showing nanofibers deposited on a glass substrate, are shown in Fig. 3. These results are representative examples from a large data base. The apparent widths of nanofibers were somewhat greater than those obtained by STEM (see Table 2) but are in agreement with the literature. Wang et al. (2006) reported a mean diameter for nanocellulose of cotton linter pulp around 90 nm, determined by the AFM technique. This suggests a tendency for side-by-side attachment in bundles, besides the effect of the tip radius of curvature and cone angle, which can increase the apparent dimensions of nanofibers. Quantitative analysis of morphological features of objects studied by AFM must allow for influence of the scanning system on the resulting image. One of the main factors limiting the accuracy of AFM images is tip-sample convolution, which is responsible for the large difference between the apparent width and height of nanofibers that are expected to be approximately round in cross section. To assess the reliability of the measured parameters, a simple one-dimensional model for tip-sample convolution was used (Garcia et al. 1998). Despite the ability to reach a high spatial resolution, AFM topographic images can sometimes not correspond to the exact surface features, owing to the creation of artifacts by the instrument. During scanning, two major AFM artifacts can appear: profile broadening, an effect of tip-sample convolution, and height lowering, due to the elastic deformation of the studied object. The latter effect is considered negligible in tapping mode, whereas the former has been the subject of numerous investigations (Allen et al. 1992; Thundat et al. 1992; Garcia et al. 1998), which have shown that, to a first approximation, the interaction between a surface feature an AFM tip, where the radius of curvature of the feature is less than that of the tip, results in an image with lateral dimensions characteristic of the tip. Thus, it can be shown that the apparent width of nanofibers arises from tip broadening (Kvien et al. 2005; Pääkko et al. 2007). In most cases, where both the very end and the wall of the tip contact the circular samples, the Garcia model (Garcia et al.

Table 2 Cotton nanofibers: average length (by STEM) and average diameter (by AFM, corrected with the Garcia model, and by STEM)

Sample	Average length (nm)	Average diameter (nm)	
	STEM	AFM (2.5 × 2.5 μm)	STEM
CNW	135 ± 50	19 ± 10	14 ± 4
CNB	140 ± 45	21 ± 9	11 ± 3
CNG	180 ± 45	24 ± 11	13 ± 2
CNR	130 ± 25	17 ± 7	10 ± 4

Results expressed as mean ± standard deviation

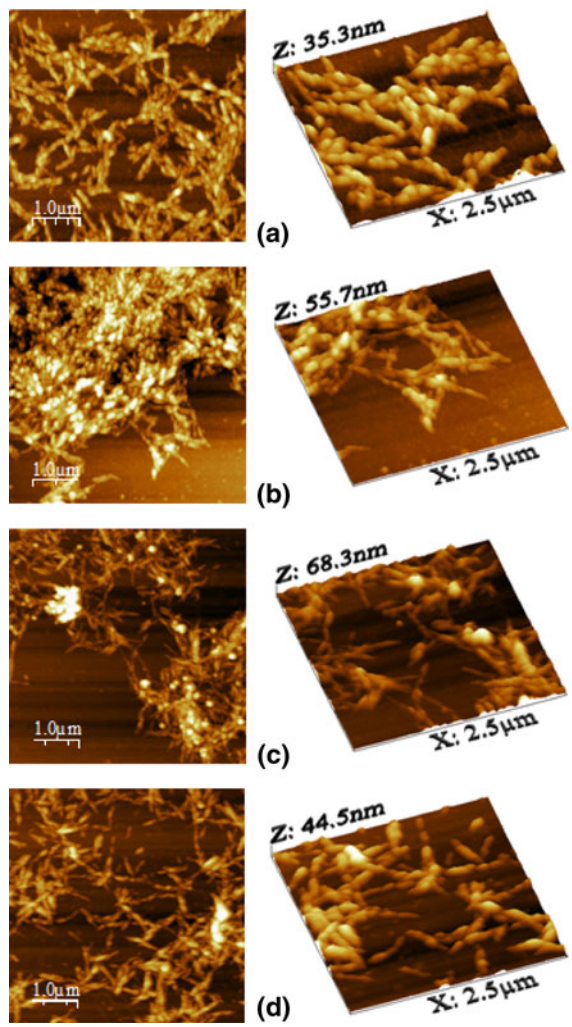

Fig. 3 AFM images of nanofibers: **a** CNW, **b** CNB, **c** CNG and **d** CNR. The AFM results indicate that the nanofibers are cylindrical and with a diameter of some nanometers

Table 3 Elemental analysis, zeta potential, crystallinity index (C_I) and initial temperature of thermal degradation (air atmosphere, Tid) for cotton fibers and respective nanofibers

Sample	Elemental analysis				Zeta potential (mV)	C_I (%)	Tid (°C)
	Nitrogen (%)	Carbon (%)	Hydrogen (%)	Sulphur (%)			
CW	0.0711	41.8379	6.3664	0	ND	77.0	320.0
CB	0.2944	41.1849	6.3550	0	ND	75.0	250.0
CG	0.3493	44.1707	6.8925	0	ND	63.0	265.0
CR	0.3585	41.6533	6.2368	0	ND	77.0	280.0
CNW	0.0733	35.8052	5.8381	2.1864	-31 ± 4	91.0	220.0
CNB	0.1369	39.3341	6.4498	1.5033	-26 ± 4	91.0	205.0
CNG	0.2648	40.9745	6.6160	1.3982	-23 ± 4	90.0	203.0
CNR	0.2587	38.7110	6.2663	1.6973	-25 ± 4	87.0	200.0

ND not determined

1998) should be applied. For an ordinary AFM tip with a radius of 11 ± 3 nm, the average dimensions obtained are presented in Table 2. The results compare well with those obtained by STEM.

The total contents of sulfur, nitrogen, carbon and hydrogen and the zeta potential (estimated as surface charge) are shown in Table 3. The total sulfur content and zeta potential were higher for CNW than for the colored nanofibers, as were the yield results presented previously. This indicates a greater incorporation of sulfate groups into the cellulose chains of the white fibers, since they have higher cellulose content (Table 1).

The X-ray diffraction patterns of the raw cotton fibers and their respective nanofibers are shown in Fig. 4. The diffractograms display a well-defined main peak around $2\theta = 22.6°$, characteristic of cellulose I (Klemm et al. 2005). In Fig. 4 it can be observed that the acid treatment results in narrow, sharper peaks for the nanofibers, because of the higher crystallinity of such nanostructures, compared to the raw fibers. The crystallinity index (C_I) was calculated and it is shown

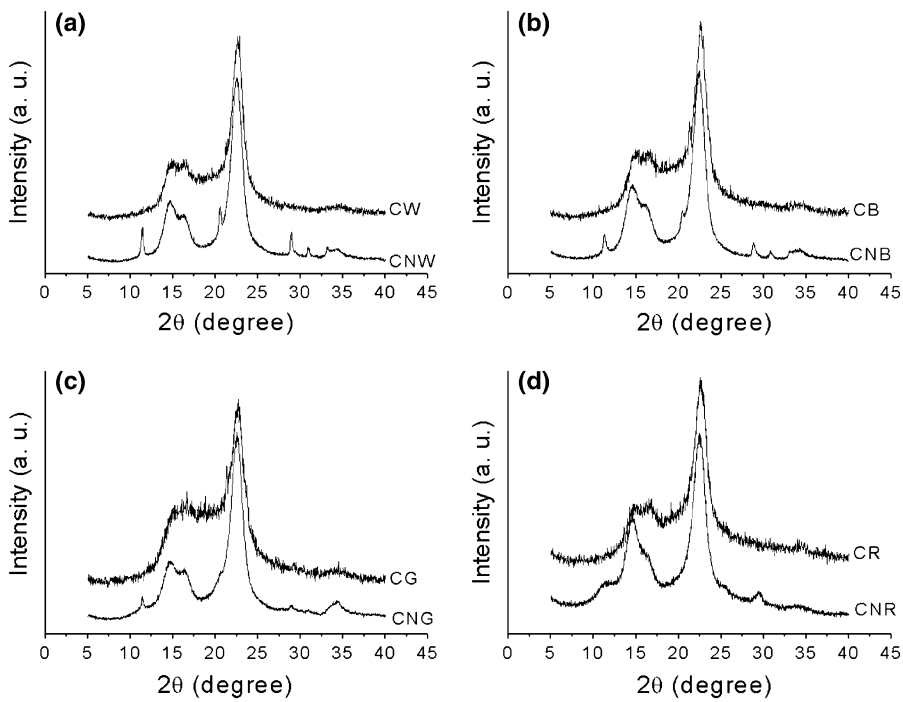

Fig. 4 X-ray diffraction patterns of raw cotton fibers and nanofibers **a**: CW and CNW, **b** CB and CNB, **c** CG and CNG and **d** CR and CNR

in Table 3, where it is seen that every cotton nanofiber had markedly higher crystallinity than its raw cotton fiber. The C_I values of nanofibers were 18% (CNW), 21% (CNB), 43% (CNG) and 13% (CNR) higher than those of their fibers. The increase in crystallinity after acid extraction of the cotton fibers is due to the different arrangements of the glucose chains in cellulose molecules (Wang et al. 2007b) after removal of the amorphous phase.

The TG curves for cotton fibers (Fig. 5a) and nanofibers (Fig. 5b) in air atmosphere show an initial small drop between 50 °C and 150 °C, which

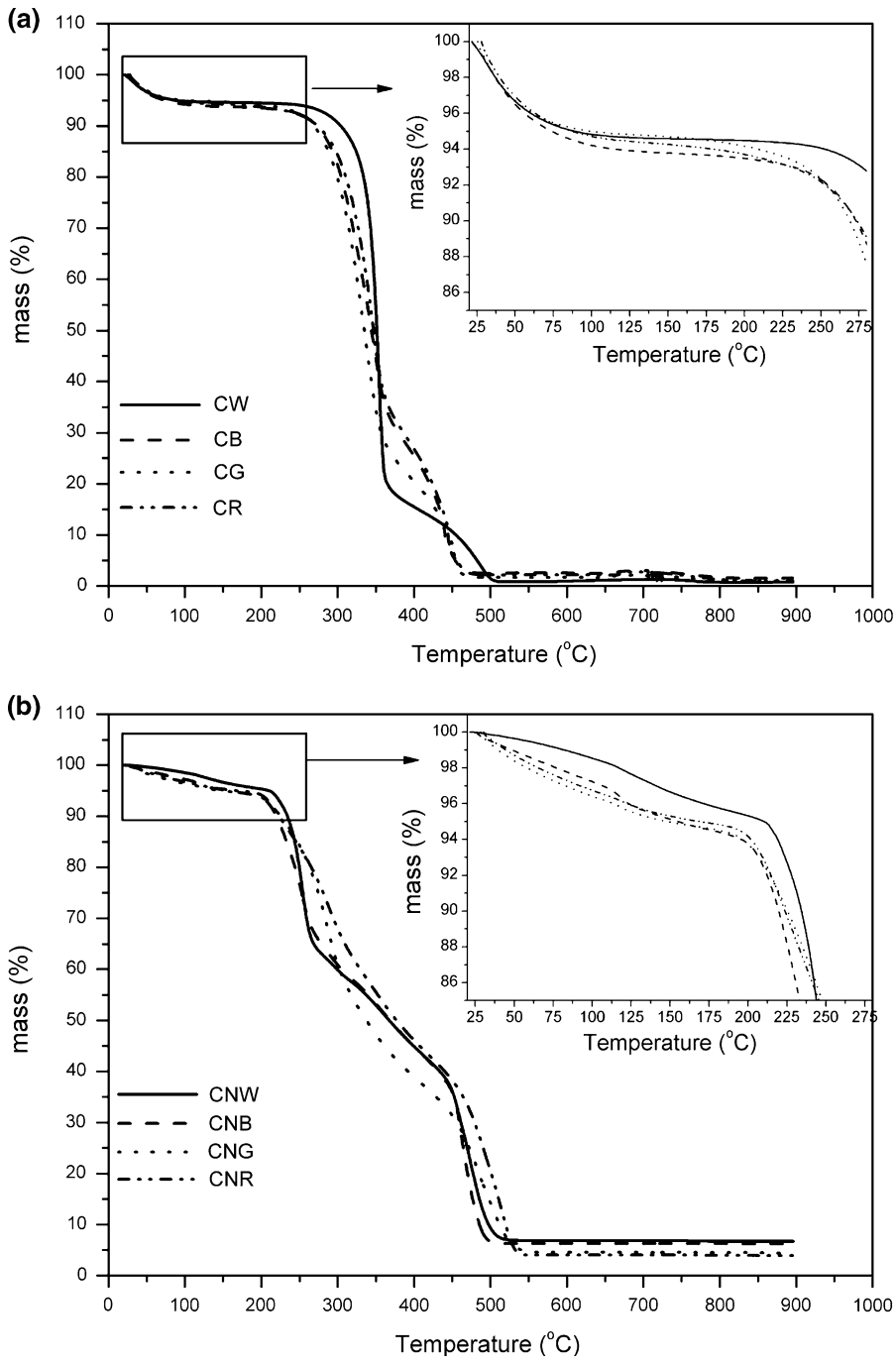

Fig. 5 TG curves of **a** raw cotton fibers and **b** their nanofibers, heated at 10 °C min^{-1} in air atmosphere

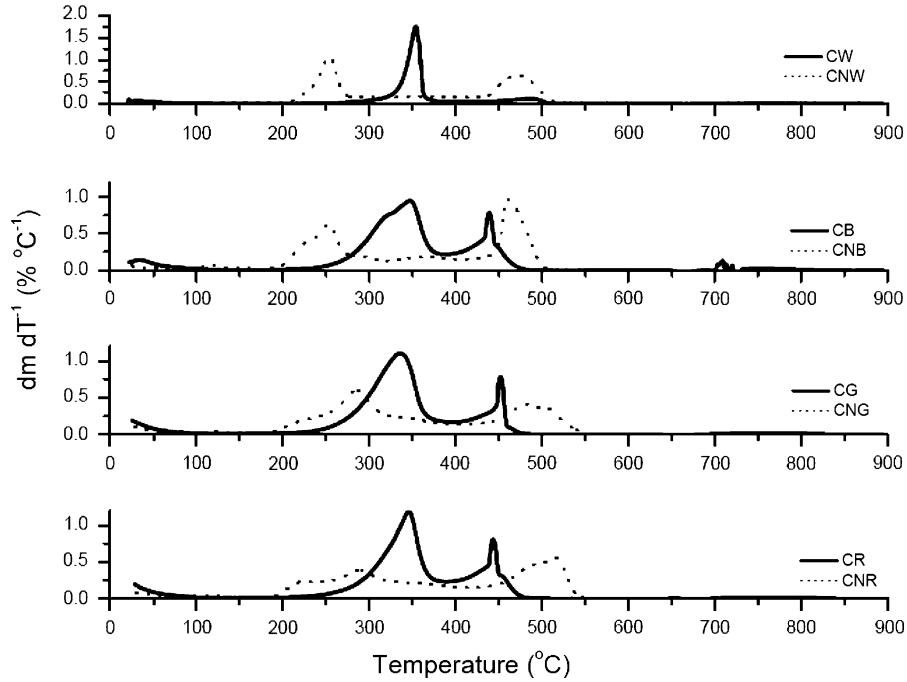

Fig. 6 The DTG curves of raw cotton fibers and (*solid lines*) their nanofibers (*dotted lines*). Analysis in air atmosphere, heated at 10 °C min^{-1}

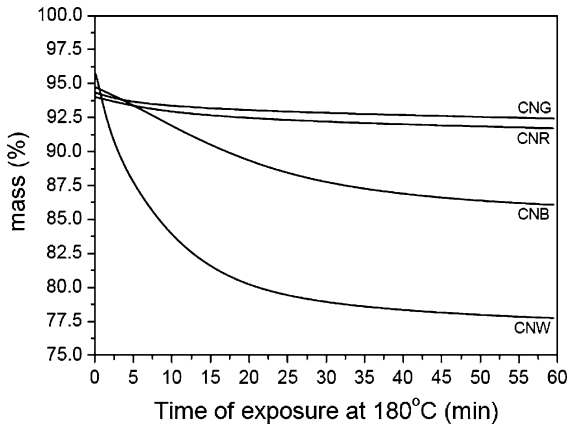

Fig. 7 The TG isotherm curves at 180 °C of cotton nanofibers. Analysis in air atmosphere, heated at 10 °C min^{-1}

corresponds to a mass loss of approximately 5% absorbed moisture. The initial temperatures of thermal degradation (T_{id}) of the samples are presented in Table 3 and were attributed to cellulose depolymerisation. In this step, the thermal degradation of nanofibers proceeded at lower temperatures than their respective raw cotton fiber. According to Roman and Winter (2004) sulfuric acid hydrolysis diminishes the thermostability of cellulose crystals. This can be observed better in DTG curves (Fig. 6). For cellulose nanofibers, the degradation reaction (200–280 °C) occurs firstly at cellulose chain units that contain sulfate groups, because they promote the dehydration reactions that release water and catalyzes the cellulose degradation reactions. Additionally, the substitution of OH groups by sulfate groups lowers the activation energy for degradation of the cellulose chain. At higher temperatures (>280 °C), the degradation reactions of the cellulose chains with lower sulfate groups contents and/or chains that did not make contact with the sulfuric acid occur (Roman and Winter 2004; Wang et al. 2007b).

The thermal stability of nanofibers held at 180 °C for 60 min is shown in Fig. 7. It is known that the exposure of polymers to an oxygen atmosphere and heating causes thermo-oxidative degradation. Figure 7 shows the higher resistance of colored nanofibers to thermal oxidation, compared to white nanofibers. This is an interesting characteristic for future applications of these nanofibers in processing polymeric nanocomposites that involves time of exposure at temperature.

Conclusions

Cellulose nanofibers from white and naturally colored cotton fibers were prepared by acid hydrolysis. No

significant morphological differences in shape and size were observed among them and between those already observed by other researching in cotton nanofibers. STEM and AFM analyses revealed that the nanofibers had a length of the 85–225 nm and diameter of 6–18 nm (by STEM measures). The nanofibers retained their original color even after acid extraction, giving colored suspensions in water. This characteristic was an interesting point because we obtain nanofiber of cellulose without pretreatment by bleaching and maintenance of the color of the suspensions after the extraction. In this way, these colored nanofiber suspensions could be tested as reinforcement for polymer matrices, with the aim of making naturally colored plastic products without the use of synthetic dyes. The main differences found were the higher extraction yield, sulfonation efficiency and initial degradation temperature of the white nanofiber under dynamic conditions of temperature. However, the colored nanofibers were thermally more stable in isothermal oxidizing conditions at 180 °C than white nanofibers.

Acknowledgments The authors gratefully acknowledge the supply of cotton fiber samples by Dr. Odilon R. R. F. Silva and Dr. Luiz P. de Carvalho (Embrapa Algodão, Brazil) and financial support provided by FAPESP (Process No. 07/50863-4), FINEP, CNPq and EMBRAPA.

References

Alemdar A, Sain M (2008) Isolation and characterization of nanofibers from agricultural residues—Wheat straw and soy hulls. Bioresour Technol 99:1664–1671

Allen MJ, Hud NV, Balooch M, Tench RJ, Siekhaus WJ, Balhorn R (1992) Tip-radius-induced artifacts in AFM images of protamine-complexed DNA fibers. Ultramicroscopy 42:1095–1100

Anglès MN, Dufresne A (2000) Plasticized starch/tunicin whiskers nanocomposites. 1. Structural analysis. Macromolecules 33:8344–8353

Anglès MN, Dufresne A (2001) Plasticized starch/tunicin whiskers nanocomposites materials. 2. Mechanical behavior. Macromolecules 34:2921–2931

Bhatnagar A, Sain M (2005) Processing of cellulose nanofibers-reinforced composites. J Reinf Plas Compos 24: 1259–1268

Buschle-Diller G, Zeronian SH (1992) Enhancing the reactivity and strength of cotton fibers. J Appl Polym Sci 45:967–979

Carvalho LP, Dos Santos JW (2003) Respostas correlacionadas do algodoeiro com a seleção para a coloração da fibra. Pesq Agropec Bras 38:79–83

Chen Y, Sun L, Cui X, Calamari Jr TA, Kimmel LB, Parikh DV (2004) Naturally colored cotton for geocomposites. In: Processing of Beltwide Cotton Conference, p 2750

Cherian BM, Pothan LA, Nguyen-Chung T, Mennig G, Kottaisamy M, Thomas S (2008) A novel method for the synthesis of cellulose nanofibril whiskers from banana fibers and characterization. J Agric Food Chem 56:5617–5627

De Rodriguez NLG, Thielemans W, Dufresne A (2006) Sisal cellulose whiskers reinforced polyvinyl acetate nanocomposites. Cellulose 13:261–270

Dong XM, Revol J-F, Gray DG (1998) Effect of microcrystallite preparation conditions on the formation of colloid crystal of cellulose. Cellulose 5:19–32

Dufresne A (2006) Comparing the mechanical properties of high performances polymer nanocomposites from biological sources. J Nanosci Nanotechnol 6:322–330

Dutt Y, Wang XD, Zhu YG, Li YY (2004) Breeding for high yield and fibre quality in coloured cotton. Plant Breed 123:141–151

Garcia VJ, Martinez L, Briceno-Valero JM, Schilling CH (1998) Dimensional Metrology of nanometric spherical particles using AFM: II, application of model-tapping mode. Probe Microsc 1:117–125

Gardner DJ, Oporto GS, Mills R, Samir MASA (2008) Adhesion and surface issues in cellulose and nanocellulose. J Adhesion Sci Technol 22:545–567

Hua S, Wang X, Yuan S, Shao M, Zhao X, Zhu S, Jiang L (2007) Characterization of pigmentation and cellulose synthesis in colored cotton fibers. Crop Sci 47:1–7

Klemm D, Heublein B, Fink HP, Bohn A (2005) Cellulose: fascinating biopolymer and sustainable raw material. Angew Chem Int Ed 44:2–37

Kvien I, Tanem BS, Oksman K (2005) Characterization of cellulose whiskers and their nanocomposites by atomic force and electron microscopy. Biomacromolecules 6:3160–3163

Lima MMS, Borsali R (2004) Rodlike cellulose microcrystals: structure, properties, and applications. Macromol Rapid Commun 25:771–787

Medeiros E, Mattoso LHC, Bernades-Filho R, Wood WJO (2008) Self-assembled films of cellulose nanofibrils and poly (*o*-ethoxyaniline). Colloid Polym Sci 286:1265–1272

Morán JI, Alvarez VA, Cyras VP, Vázquez A (2008) Extraction of cellulose and preparation of nanocellulose from sisal fibers. Cellulose 15:149–159

Murthy MSS (2001) Never say dye: the story of coloured cotton. Resonance 6:29–35

Nakagaito AN, Iwamoto S, Yano H (2005) Bacterial cellulose: the ultimate nano-scalar cellulose morphology for the production of high-strength composites. Appl Phys A Mat Mater Sci Process 80:93–97

Orts WJ, Shey J, Iman SH, Glenn GM, Guttman ME, Revol J-F (2005) Application of cellulose microfibrils in polymer nanocomposites. J Polym Environ 13:301–306

Pääkko M, Ankerfors M, Kosonen H, Nykänen A, Ahola S, Österberg M, Ruokolainen J, Laine J, Larsson PT, Ikkala O, Lindström T (2007) Enzymatic hydrolysis combined with mechanical shearing and high-pressure. Biomacromolecules 8:1934–1941

Pu YQ, Zhang JG, Elder T, Deng Y, Gatenholm P, Ragauskas AJ (2007) Investigation into nanocellulosics versus acacia reinforced acrylic films. Compos Part B-Eng 38:360–366

Rocha MS, Carvalho JMFC, Mata MERMC, Lopes KP (2008) Indução de superbrotamento e regeneração de plantas in

vitro, nas cultivares de algodão colorido. R Bras Eng Agric Ambiental 12:503–506

Rodgers J, Thibodeaux D, Cui X, Martin V, Watson M, Knowlton J (2008) Instrumental and operational impacts on spectrophotometer color measurements. J Cotton Sci 12:287–297

Roman M, Winter WT (2004) Effect of sulfate groups from sulfuric acid hydrolysis on the thermal degradation behavior of bacterial cellulose. Biomacromolecules 5:1671–1677

Samir MASA, Alloin F, Dufresne A (2005) Review of recent research into cellulosic whiskers, their properties and their application in nanocomposite field source. Biomacromolecules 6:612–626

Thundat T, Zheng X-Y, Sharp SI, Allison DP, Warmack BJ, Joy DC, Ferrell TL (1992) Calibration of atomic force microscope tips using biomolecules. Scanning Microsc 6:903–910

Wang Y, Cao X, Zhang L (2006) Effects of cellulose whiskers on properties of soy protein thermoplastics. Macromol Biosci 6:524–531

Wang N, Ding E, Cheng R (2007a) Thermal degradation behavior of spherical cellulose nanocrystals with sulfate groups. Polymer 48:3486–3493

Wang B, Sain M, Oksman K (2007b) Study of structural morphology of hemp fiber from the micro to the nanoscale. Appl Compos Mater 14:89–103

Xiao YH, Zhang Z-S, Yin M-H, Luo M, Li X-B, Hou L, Pei Y (2007) Cotton flavonoid structural genes related to the pigmentation in brown fibers. Biochem Biophys Res Commun 358:73–78

Zhang JG, Elder TJ, Pu YQ, Ragauskas AJ (2007) Facile synthesis of spherical cellulose nanoparticles. Carbohydr Polym 69:607–611

Zhang J, Jiang N, Dang Z, Elder TJ, Ragauskas AJ (2008) Oxidation and sulfonation of cellulosic. Cellulose 15: 489–496

Zhu S-E, Gao P, Sun J-S, Wang H-H, Luo X-M, Jiao M-Y, Wang Z-Y, Xia G-X (2006) Genetic transformation of green-colored cotton. In vitro Cell Dev Biol Plant 42: 439–444

Zuluaga R, Putaux JL, Restrepo A, Mondragon I, Gañán P (2007) Cellulose microfibrils from banana farming residues: isolation and characterization. Cellulose 14: 585–592